

*Scientific paper*

## Self-Healing Capability of Fibre Reinforced Cementitious Composites

Daisuke Homma<sup>1</sup>, Hirozo Mihashi<sup>2</sup> and Tomoya Nishiwaki<sup>3</sup>

Received 23 February 2009, accepted 8 May 2009

### Abstract

In order to investigate the self-healing capability of fibre reinforced cementitious composites (FRCC), mechanical properties and surface morphology of crack in FRCC were studied. Three types of FRCC specimens containing (1) polyethylene (PE) fibre, (2) steel cord (SC) fibre, and (3) hybrid fibres composite (both of PE and SC) were prepared. These specimens, in which cracks were introduced by tension test, were retained in water for 28 days. The self-healing capability of the specimens was investigated by means of microscope observation, water permeability test, tension test and backscattered electron image analysis. It was found that many very fine fibres of PE were bridging over the crack and crystallization products became easy to be attached to a large number of PE fibres. As a result, water permeability coefficient decreased and tensile strength was improved significantly. Therefore amount of the PE fibre per volume was indicated to have a great influence on self-healing. Furthermore, by means of backscattered electron image analysis, it was also shown that the difference of hydration degree in each FRCC has only little influence on the self-healing capability in case of the employed test series.

### 1. Introduction

Cracking is inherent in reinforced concrete (RC) structures and leads to serious damage in service period. Cracking is caused by various sources such as drying shrinkage, external force and freezing and thawing. No matter what the reason, the crack in RC structures allows the early access of aggressive agents (like chloride ions and CO<sub>2</sub>), and as a result the reinforcement's corrosion occurs at an early age. This corrosion brings not only the decrease of strength, but also the expansion of the reinforcement that enlarges the crack width and causes spalling of the cover concrete. So we have to avoid this cracking in RC structures as much as possible. One of the most popular and widely used technique to address this problem is the use of short fibres. The randomly distributed fibres bridge over cracks and are able to decrease the crack width and to block aggressive agent. Research results and design code indicate that about 0.1 mm or smaller width crack is relatively safe due to self-healing autogenously caused by immersing moisture (e.g. Edvardsen 1999). In this self-healing phenomenon, FRCC that enables to keep the crack width smaller can be greatly effective.

Since considerable improvement in the post-cracking behaviour of concrete containing fibres is achieved, FRCC has been widely used since the middle of 20<sup>th</sup> century. Even recently fundamental studies about the

mechanisms of toughening which may contribute to further development of advanced FRCC were presented (for example, Fantilli *et al.* 2007; Dick-Nielsen *et al.* 2007; Yang *et al.* 2008). In the meanwhile, some works of practical application of FRCC for developing high performance structural members were presented, too. Some studies on ductile high strength concrete columns toughened by containing steel fibre were reported (Sharma *et al.* 2007; Sugano *et al.* 2007; Kimura *et al.* 2007). Ultra ductile fibre reinforced cementitious composites (so called strain hardening cementitious composite: SHCC) have been also developed (Li 2003; Kanda and Li 2006) and a simplified inverse method for determining the tensile properties of SHCC that is essential for quality control in practice was proposed (Qian and Li 2007; Qian and Li 2008).

Self-healing, in another word autogenous healing, of concrete and reinforced concrete is a phenomenon that has been often studied by many researchers (for example, Ramm and Biscopig 1998; Li *et al.* 1998; Edvardsen 1999; Reinhardt and Jooss 2003; Yang *et al.* 2005; Heide and Schlangen 2007; Granger *et al.* 2007). Many experimental results and practical experiences have demonstrated that cracks in concrete have the ability to heal themselves and water flow through cracks was reduced with time. The following reasons for the self-healing have been cited (Ramm and Biscopig 1998): 1) further reaction of the unhydrated cement; 2) expansion of the concrete in the crack flanks; 3) crystallization of calcium carbonate; 4) closing of the cracks by solid matter in the water; 5) closing of the cracks by spalling-off loose concrete particles resulting from the cracking. Among these reasons, however, it was clarified that crystallization of calcium carbonate within the crack was the main mechanism for self-healing of matured concrete (Edvardsen 1999). It was also reported

<sup>1</sup>Graduate student, Dept. of Architecture and Building Science, Tohoku University, Japan.

<sup>2</sup>Professor, Dept. of Architecture and Building Science, Tohoku University, Japan.

*E-mail:* mihashi@timos.str.archi.tohoku.ac.jp

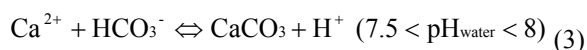
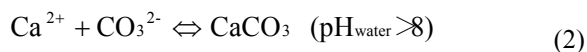
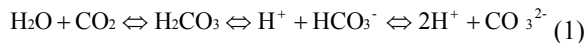
<sup>3</sup>Associate Professor, Faculty of Education, Art and Science, Yamagata University, Japan.

that the growth rate of calcium carbonate within the crack was dependent on crack width and water pressure, but that it was independent of concrete composition (type of cement and aggregate) and type of water (i.e. hardness of water). On the other hand, Granger *et al.* (2007) carried out an experimental program of mechanical test on ultra high performance concrete and concluded that the self-healing of the pre-existing crack was mainly due to hydration of anhydrous clinker on the crack surface and that the stiffness of newly formed crystals is close to that of primary C-S-H. While there are many studies of self-healing of concrete, there are quite few of such studies on FRCC. Li *et al.* (1998) carried out experimental studies on self-healing capability of SHCC and concluded that self-healing of the induced micro cracks was observed not only by formation of a distinct deposit inside the cracks but also by almost complete recovery of the pre-cracking stiffness. Homma *et al.* (2008a, 2008b) reported the summary of a series of experimental study on the self-healing capability of FRCC.

In this paper, the experimental study of the FRCC's self-healing capability is reported. The capability is evaluated by water permeability test, microscope measurement, tension test and backscattered electron image.

## 2. Self-healing

Self-healing is the natural process of crack repair that can occur in concrete in the presence of moisture. The deposition of calcium carbonate is said to be generated according to the following reactions (Edvardsen 1999).



The carbon dioxide  $\text{CO}_2$  in the air is dissolved in water and the calcium ion  $\text{Ca}^{2+}$  is derived from concrete. These  $\text{CO}_2$  and  $\text{Ca}^{2+}$  are combined with each other to produce calcium carbonate crystals. Then the calcium carbonate crystallization made in this way is attached to crack surface and fibers. As a result, crack width is reduced and after a certain time the crack is repaired.

## 3. Experimental procedure

In this study, the self-healing capability is evaluated by the microscope observation, water permeability test, tension test and backscattered electron image analysis. **Table 1** shows the employed materials and **Table 2** shows the mix proportions together with the fresh property. In this study three types of FRCC were studied: (1) containing micro polyethylene fibre ( $\phi=12\mu\text{m}$ , length=6mm) (FRCC(PE)), (2) containing steel cord fibre ( $\phi=0.4\text{mm}$ , length=32mm) (FRCC(SC)), and (3) containing both of PE and SC fibres (i.e. hybrid fibre

Table 1 Employed materials in this study.

Cement	High-early-strength Portland cement	$\rho = 3.14 \text{ g/cc}$
Aggregate	Silica sand (no.7)	$\rho = 2.61 \text{ g/cc}$ Diameter: 180 $\mu\text{m}$
Mixing Materials	Silica fume	$\rho = 2.2 \text{ g/cc}$ Diameter: 0.15 $\mu\text{m}$
Viscous Agent	Water-soluble cellulose	$\rho = 1.1 \text{ g/cc}$
Fiber	Polyethylene (PE)	Mentioned below
	Steel cord (SC)	Mentioned below
Screw Bar	Steel screw bar	Nominal diameter: 6mm (M6)



PE fiber (length=6<sup>mm</sup>)



SC fiber (length=32<sup>mm</sup>)

Types of Fiber	Length (mm)	Diameter (mm)	Modulus (GPa)	Tensile strength (MPa)	Density (g/cc)
PE fiber	6	0.012	73	2580	0.97
SC fiber	32	0.4	200	2850	7.84

Table 2 Mix proportion of FRCC specimens investigated in this paper.

Types of Mix	Water/Binder	Sand/Binder	Silica fume/Binder	SP/Binder	PE fiber (Vol. %)	SC fiber (Vol. %)	fiber content (piece/m <sup>3</sup> )
FRCC(SC)	0.45	0.45	0.15	-	-	0.75	187 $\times 10^4$
FRCC(PE)				0.09	1.5	-	221 $\times 10^8$
HFRCC				0.09	0.75	0.75	111 $\times 10^8$

Note: Binder = Cement + Silica fume; SP = Superplasticizer (Polycarboxylate)

Types of Mix	Table flow (cm $\times$ cm)	Air content (%)
FRCC(SC)	16.3 $\times$ 16.0	0.90
FRCC(PE)	13.6 $\times$ 13.8	5.13
HFRCC	14.7 $\times$ 14.7	3.36

composite: HFRCC).

In all series, four specimens of 25 $\times$ 75 $\times$ 75[mm] were prepared. After standard curing for one week, cracks were introduced in each specimen by means of a uni-axial tension test. **Figure 1** shows the outline of the tension test. During this test, each specimen was stretched to different strain levels in order to have different maximum crack width. In **Fig. 2**, the relations between elongation and stress under uni-axial tension are shown. The nonlinearity is corresponding to the accumulation of multiple cracking. After the tension test, the

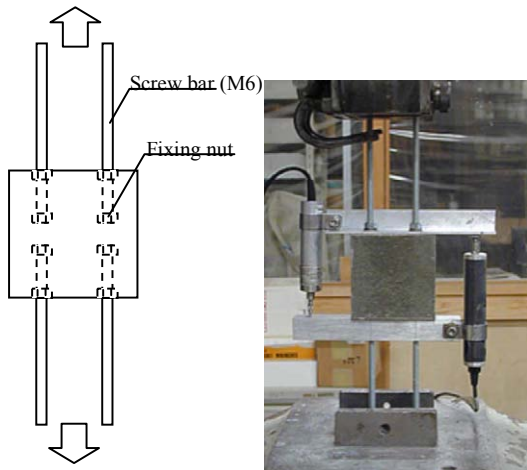


Fig. 1 Test set-up of uni-axial tension test.

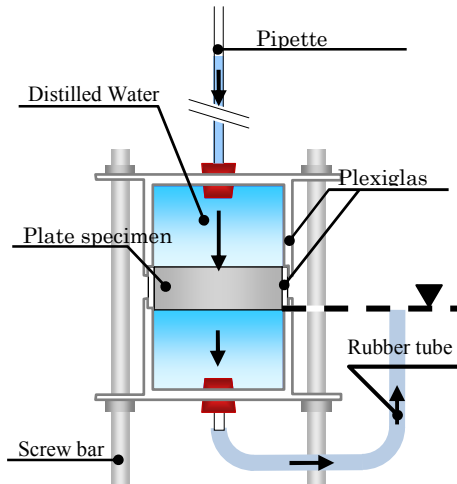
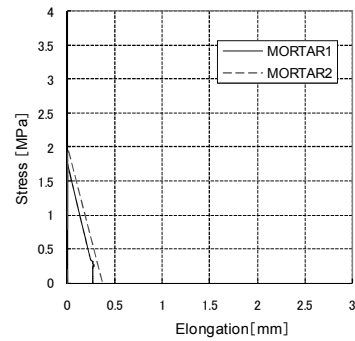


Fig. 3 Schematic description of water permeability test.

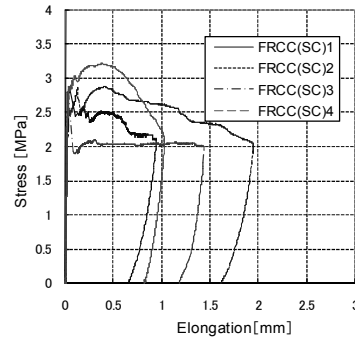
Table 3 Maximum crack width evaluated by means of microscope observation in the permeability test specimens. (unit : mm)

		No. of specimens			
		No. 1	No. 2	No. 3	No.4
Type of mixes	FRCC(SC)	0.035	0.076	0.088	0.757
	FRCC(PE)	0.019	0.038	0.119	0.368
	HFRCC	0.017	0.081	0.407	0.71

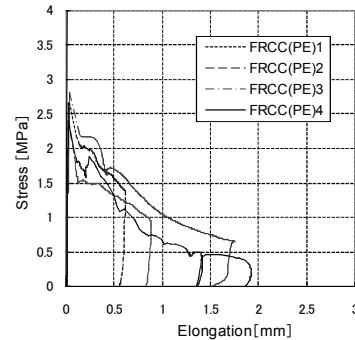
crack surface was observed by means of a digital microscope and the crack width was measured as shown in Table 3. These values were obtained on the inlet side of permeability test specimens, while microscopic observation to measure the thickness of crystallization products was carried out on both sides of each specimen. As shown in 4.2, the permeability coefficient is a function of  $w^3$ . Therefore only one crack of the maximum width on the inlet side among the multiple cracks is dominant for the water permeability. After the microscope observation,



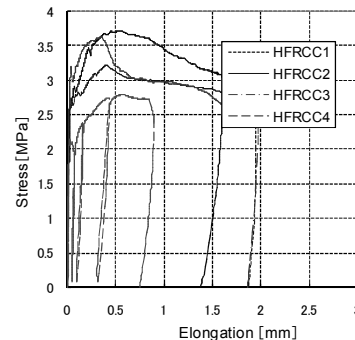
MORTAR



FRCC(SC)



FRCC(PE)



HFRCC

Fig. 2 Retation between elongation and stress under uni-axial tension.

the specimens were tested for water permeability. The schematic description of the water permeability test

(Nishiwaki and Mihashi 2003) is shown in **Fig. 3**. The water permeability coefficient was evaluated by the water flow speed through the plate specimen. After the water permeability test, all specimens were kept for 28 days in water tank of 20°C which is usually used for standard curing. In order to investigate the effect of the self-healing of crack, water permeability tests and microscopic measurement were conducted again at 3, 14 and 28 days. After 28 days, the uni-axial tension test was performed again, too.

## 4. Experimental Results and Discussion

### 4.1 Microscopic observation

The formation of crystallization products (**Fig. 4**) that might be the source of self-healing was monitored just after the tension test and at the end of 3, 14, and 28 days after water permeability test. Additionally the thickness of the crystallization products on the crack surface was also measured by means of a digital microscope. **Table 4** shows the typical crack surface photographs in FRCC (PE), FRCC (SC), and HFRCC at the elapsed time of 0 day (immediately after tension test and before immersion in water), at 3 days, 14 days and 28 days.

The reason why some values of the maximum crack width are different from ones shown in **Table 3** is that not only the inlet side for water permeability test but both sides of each specimen were observed by the digital microscope for measuring the crack width and the thickness of crystallization products. It can be clearly seen in **Table 4** that the crack surface of all specimens immediately after tension test is clear and there are no chemical products on the surface. At 3 days, however, in the crack surfaces of FRCC(PE) and HFRCC, many crystallization products were confirmed to be attached and this attachment is done not only to crack surface but also to many PE fibres. Furthermore in FRCC(PE), even though crack width reached 100µm, crack was confirmed to be repaired by the crystallization products attached to many fibres bridging the crack. However in the place of little fibre bridging, especially in almost all FRCC(SC), the



Fig. 4 Example of crystallization products.

deposition of crystallization products was not seen. Even if there were fibres bridging the crack, in the case when crack width was too wide and PE fibres were dropped out, little attachments of the crystallization products could be confirmed. After 3 days, in FRCC(PE) and HFRCC, the thickness of crystallization products attached to the crack surface and PE fibres increased as the time advanced. However, in FRCC(SC), the crack surface remained to be clear. Therefore it can be concluded that amount of the PE fibres per volume has a great influence on the self-healing.

After 3 days, it was also observed that steel cords on the crack surface in FRCC(SC) and HFRCC corroded and the volume expanded.

**Figure 5** shows the time dependence of mean thickness of the crystallization products attached to the crack surface (summation of products thickness on both sides of the crack surface). The increasing rate of the mean thickness during the first 3 days is higher than that after 3 days. This could be because  $Ca^{2+}$  diffusion speed from the inside of FRCC was reduced as the time advanced since the formation of the crystallization product layer may prevent the diffusion (Edvardsen 1999). Order of the amount of the attached products in each FRCC material was FRCC(SC) < HFRCC < FRCC (PE). This order is corresponding to that of the piece number of mixed fibres per unit volume shown in **Table 2** (i.e. FRCC(SC) < HFRCC < FRCC (PE)). Therefore it can be concluded that the piece number of mixed fibre per unit volume has the dominant influence on the thickness of the crystallization products attached to the crack surface.

**Figure 6** shows the relationship between the maximum crack width and the mean attachment thickness at 28 days. In each type of mix, totally 8 data of the maximum crack width measured from both sides of each specimen are plotted. In this figure, when the slope of regression line equals to 1, the attachment thickness is thought to reach the crack width and it can be said that the crack was repaired. According to the results shown in this figure, when crack width is less than 100µm, the

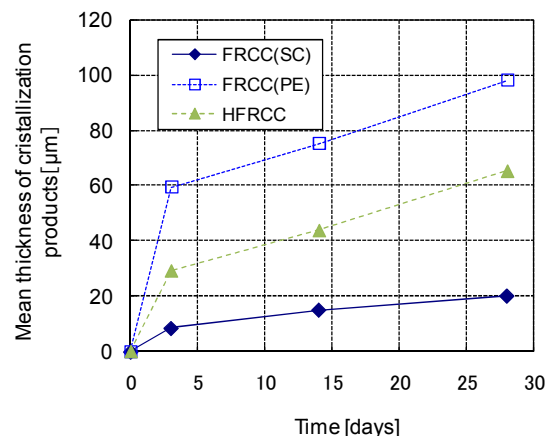


Fig. 5 Time dependence of mean thickness of crystallization products attached to the crack surface.

Table 4 Microscopic observation of crystallization products at a crack surface.

	Elapsed time (day)			
	0*	3	14	28
FRCC (SC) Steelcord fiber speci- men No. 2 (crack width: 1.976mm)				
FRCC (PE) Polyethylene fiber speci- men No. 4 (crack width: 0.368mm)				
HFRCC Steel-PE hybrid fiber specimen No. 1 (crack width: 1.532mm)				

\* Immediately after tension test before immersion in water.

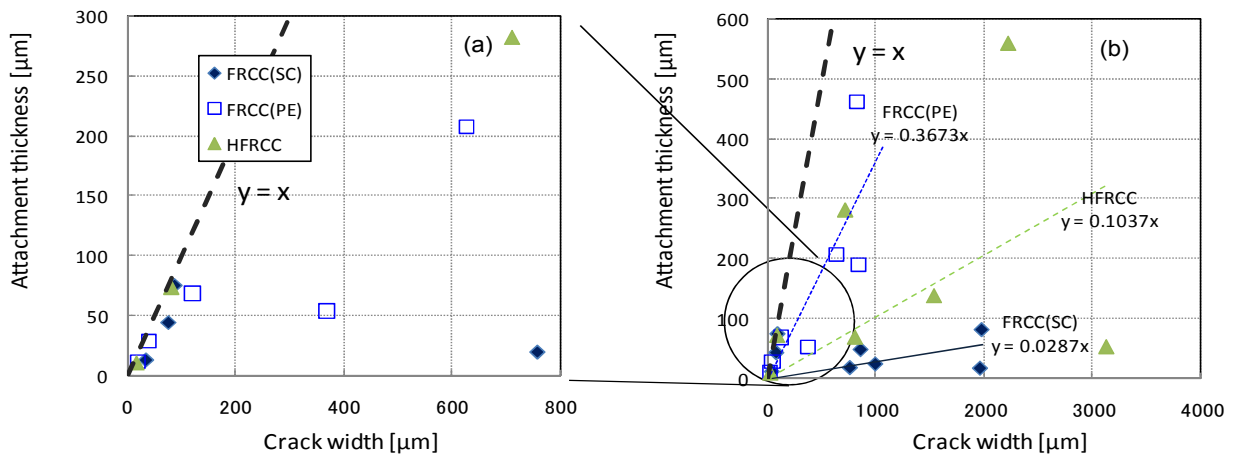


Fig. 6 Relationship between the maximum crack width and the mean thickness of crystallization products observed on each specimens surface .

slope was close to 1 and crack was repaired easily in each series. However, when crack width is wider than 100μm, the slopes of the regression lines are much lower than 1. Among these three regression lines shown in Fig. 6(b), the slope of FRCC(PE) is highest. It confirms that FRCC(PE) is repaired most easily.

**4.2 Water permeability test**

The water permeability coefficient was calculated as follows. Since the water flow in this study is assumed to be continuous through the laminar, Darcy’s law can be

applied. Darcy’s law states:

$$Q = kA \frac{h}{l} \tag{1}$$

where  $Q$  = the flow rate through the specimen ( $dV/dt$ );  $V$  = the total volume of water that travels through the sample;  $k$  = the water permeability coefficient and the parameter under this study,  $l$  = the thickness of the specimen, and  $A$  = the surface area of the plate specimen.

Then, because the flow is continuous, the amount of

water flowing out of the pipe is given by Equation (2):

$$\frac{dV}{dt} = -A' \left( \frac{dh}{dt} \right) \tag{2}$$

where  $dh/dt$  = the differential of pressure between the initial pressure head  $h_0$  and the remaining pressure head  $h_1$  at the measured time  $t$ ;  $A'$  = the cross-sectional area of the pipe.

By combining Equations (1) and (2), Equation (3) is obtained.

$$k \frac{h}{l} A = - \frac{A' dh}{dt} \tag{3}$$

By integrating Equation (3), Equation (4) is obtained.

$$k \int_0^t dt = -l \frac{A'}{A} \int_{h_0}^{h_1} \frac{dh}{h} \tag{4}$$

The water permeability coefficient is finally given by Equation (5).

$$k = l \frac{A'}{At} \ln \frac{h_0}{h_1} \tag{5}$$

By the use of this coefficient of water permeability, the self-healing capability of each FRCC was evaluated.

**Figure 7** shows the relationship between the coefficient of water permeability and residual elongation just after the tension test. The coefficient of water permeability tends to increase as residual elongation increases, but this tendency is quite variable and dependent on the type of fibre. This could be because the residual elongation doesn't indicate the maximum crack width but reflects the summation of crack widths and fibre reinforced cementitious composites make multiple cracking generated.

In the meanwhile, **Fig. 8** shows the relationship between the coefficient of water permeability and the maximum crack width just after the tension test without any self-healing. In addition to four data obtained from four specimens of each type of mix, some data of HFRCC obtained in a preliminary test are also plotted. In the figure, regression curves based on the following equation are also shown, which was obtained according to a parallel board theory of fluid dynamics (Tsukamoto and Woener 1991).

$$k = \frac{a l g}{12 \nu} w^3 \tag{6}$$

where  $w$  : crack width [mm];  $a$  : flow rate coefficient indicating smoothness of crack surface ( $0 < a \leq 1$ ) to estimate the influence of the crack geometry;  $l$  : pressure gradient ( $h/d$ );  $h$  : height of fluid column on the inlet side;  $d$  : length of crack in flow direction;  $\nu$  : kinematic viscosity [ $m^2/s$ ];  $g$  : gravity acceleration.  $l$  : length of crack at a right angle to the flow direction [m].

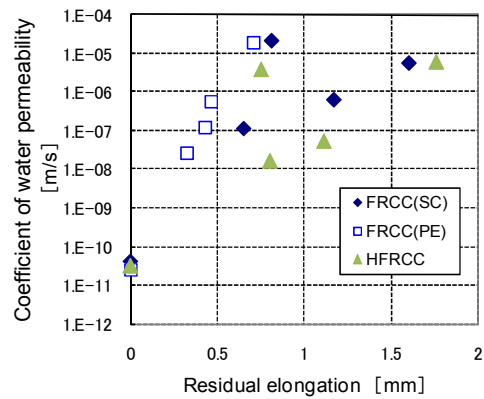


Fig. 7 Relationship between the coefficient of water permeability and residual elongation.

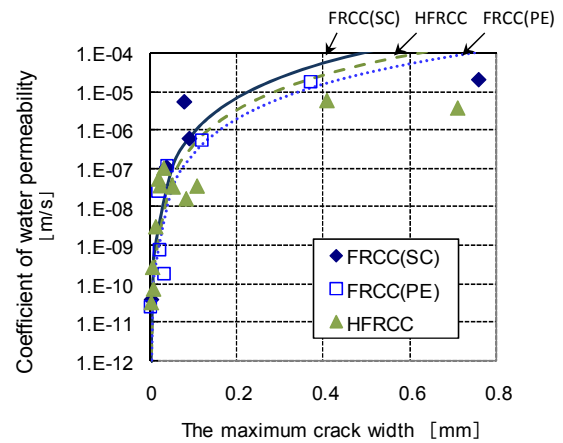


Fig. 8 Relationship between the coefficient of water permeability and the maximum crack width.

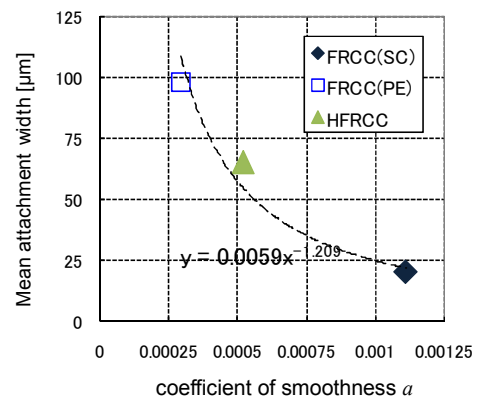


Fig. 9 Relationship between the coefficient of smoothness and mean attachment thickness.

From Equation (6), the coefficient of water permeability is proportional to cube of crack width:  $w$  and the coefficient  $a$ . The result of **Fig. 8** is corresponding to this theory basically. This tendency, however, also has variability in the small range of the maximum crack width

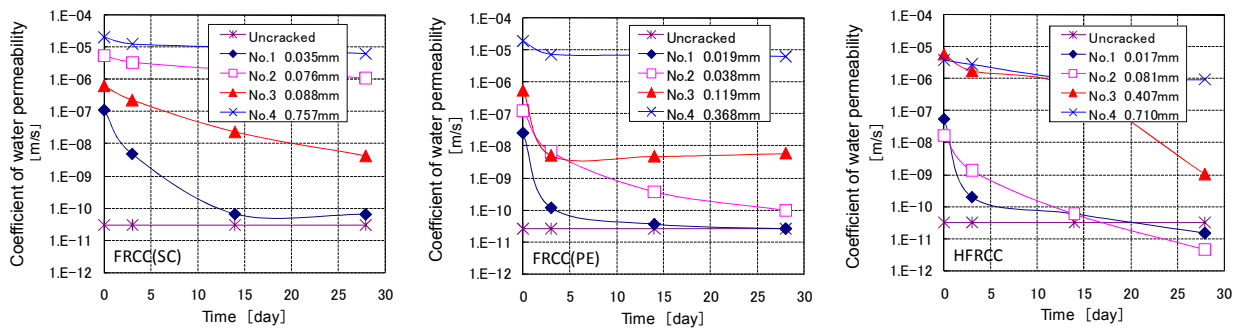


Fig. 10 Time dependence of water permeability coefficient in each FRCC.

where crack width is less than 0.1mm and it may mean that the simple parallel board theory can't be applied in the range where elongation is small. This is because fibre reinforced cementitious composites generically make multiple crack in the range of small elongation.

**Figure 9** shows the relationship between the coefficient indicating the smoothness of crack surface and attachment thickness at 28 days. From this figure, it was confirmed that as the surface crack becomes smoother, the thickness of the attachment becomes thinner. This could be because attaching of crystallization products on crack surface becomes difficult due to no or little PE fibres remained on the crack surface. Therefore the smoothness of crack surface is thought to have strong influence on the self-healing.

**Figure 10** shows the result of the water permeability test of the cracked and uncracked specimens. As can be seen in this figure, the coefficient of water permeability for all specimens decreased until 3 days except the uncracked specimens. However, after 3 days the decreasing rate of the coefficient of water permeability slowed down significantly in all specimens. This corresponds to the microscopic observation results shown in **Fig. 5** in which the crystallization products attaching speed is faster until 3 days than after 3 days. It can also be noticed that, in the specimens with a wider crack, the coefficient of water permeability was almost constant after 3 days. It means that the crystallization products are the source of the self-healing mechanism but that the mechanism doesn't work well in wider cracks. On the other hand, in case of specimens with a smaller crack width, the coefficient of water permeability decreased as time advances even after 3 days and in some cases reached to the same values to those obtained in uncracked specimens. This clearly indicates that, in such a small crack width, the crystallization products have a great effect on self-healing of crack. **Figure 11** shows the influence of time dependence of water permeability coefficient due to type of FRCC. The decrease of the water permeability coefficient in FRCC(PE) and HFRCC is more than that in FRCC(SC). This can be because the self-healing products could attach to the crack surface more in FRCC(PE) and HFRCC than in FRCC(SC).

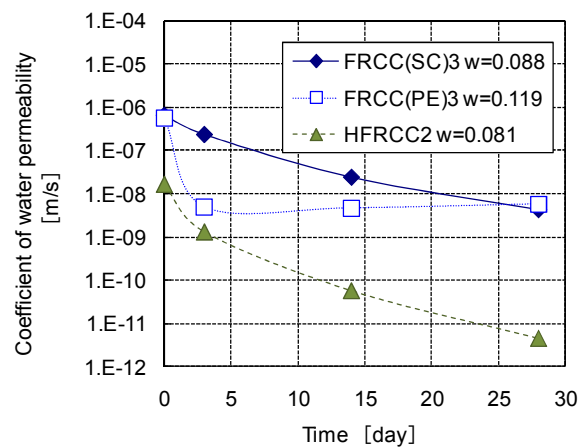


Fig. 11 Influence of time dependence of water permeability coefficient due to type of FRCC.

### 4.3 Raman spectroscopy analysis

In order to examine the chemical composition of the crystallization products that is the source of self-healing of crack, FRCC(PE) specimens were analysed by Raman spectroscopy. **Figure 12** shows the Raman spectroscopy of FRCC (PE) samples. In this figure, upper, middle, and lower profiles were taken from uncracked area, cracked area, and pure calcium carbonate crystals, respectively. It can be seen from this figure that the peaks of cracked area coincide with those of pure calcium carbonate crystal. On the other hand, in the case of uncracked area, such a peak couldn't be observed. Therefore the formation of crystallization products, that is, the formation of self-healing products in FRCC was confirmed to be calcium carbonate crystals.

### 4.4 Uni-axial tension test of self-healed specimens

In order to evaluate the effect of self-healing on the tensile properties, the self-healed FRCC specimens were tested by uni-axial tension test again. **Figure 13** shows the typical relations between tensile stress and elongation before and after the self-healing. **Figure 14** shows the schematic description of general tensile stress-elongation

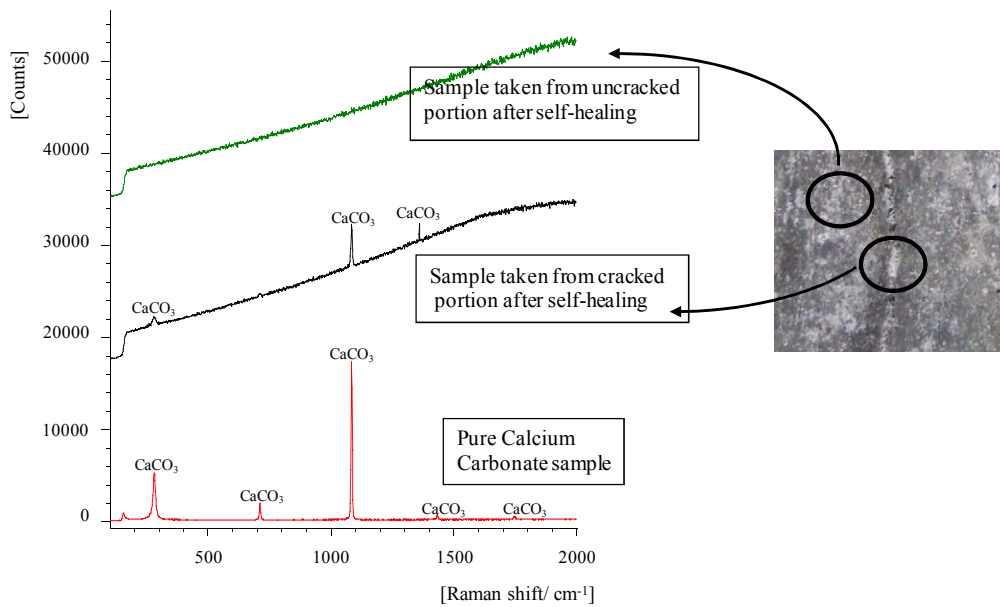


Fig. 12 Raman spectroscopy of FRCC (PE) specimens.

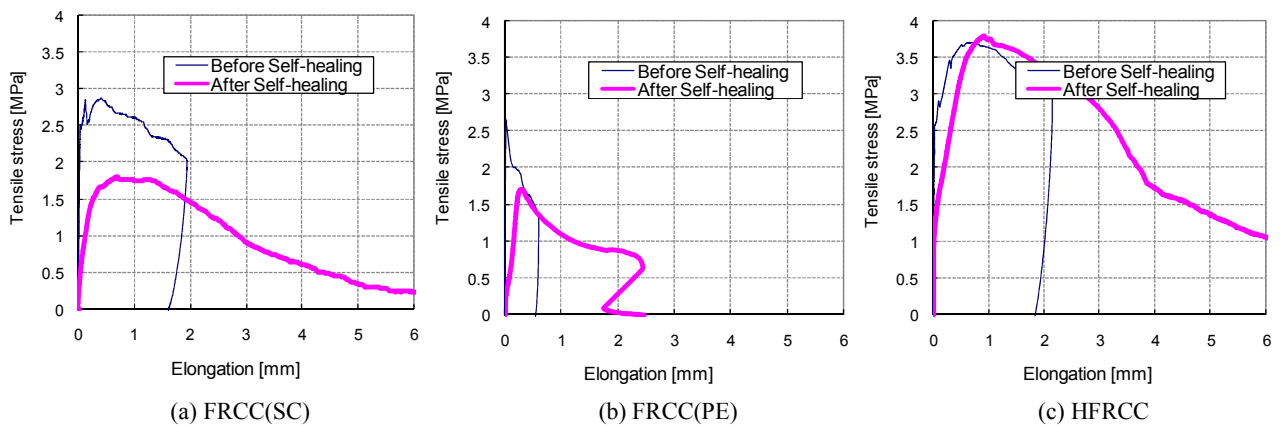


Fig. 13 Comparison of tensile property of specimens before and after 28 days of self-healing.

response of FRCC. In case of FRCC(PE), specimens showed a tendency of quasi-brittle fracture because the length of the used polyethylene fibres was short. After the first crack occurred, tensile stress soon decreased accompanying the strain softening behaviour. Multiple cracking was observed in the range of small strain, though a dominant crack was localized as the strain increased. In case of HFRCC, the length of steel cord had the concavity and convexity to create the high bond strength while the short polyethylene fibres made the matrix tough enough to prevent the spalling of matrix when the steel cord was pulled out from the crack surface (Mihashi and Kohno 2007). As a result, HFRCC showed a very ductile stress versus elongation relation. Multiple cracking was observed but finally a dominant crack was localized as observed in FRCC (PE). FRCC (SC) specimens which contained only steel cord showed lower strength and a little less ductility than those of HFRCC.

This is because FRCC (SC) didn't contain any polyethylene fibres. In case of FRCC (SC), some specimens showed multiple cracking in a small strain range but the others didn't. While there was a scatter in the cracking behaviour in the small strain range, a dominant crack was easily localized in any cases.

In order to compare the strength recovery due to the self-healing of each FRCC specimen, the strength recovery rate ( $c$ ) was defined as follows:

$$c = \frac{\sigma_2 - \sigma_0}{\sigma_1 - \sigma_0} \times 100 \quad (6)$$

where  $\sigma_0$  = the stress at the unloading in the first tension test,  $\sigma_1$  = the tensile strength in the first tension test, and  $\sigma_2$  = the tensile strength after the self-healing.

By use of this  $c$ , it can be possible to judge the recovering capability of the strength in each FRCC as follows.

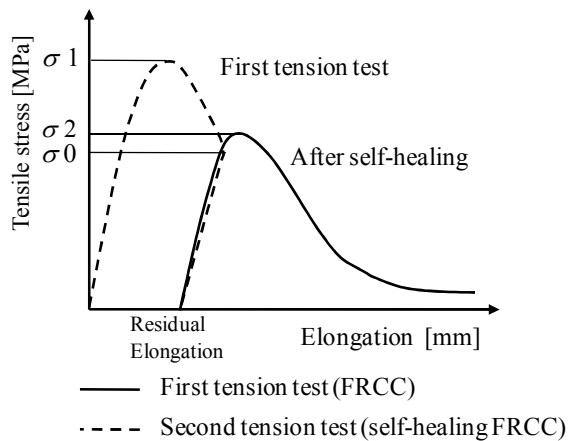


Fig. 14 Schematic of the relationship between tensile stress and tensile elongation of FRCC.

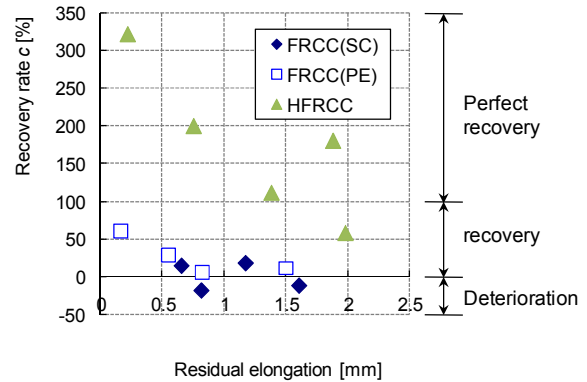


Fig. 15 Relationship between recovery rate and residual elongation.



Fig. 16 Comparison of crack surface after second tension test.

If  $c$  is over 100, this specimen can be considered to be recovered perfectly. If  $c$  is over 0 and under 100, this one was recovered a little. If  $c$  is equal to 0, this one was not recovered. If  $c$  is under 0, this one was deteriorated. **Figure 15** shows the relationship between the strength recovery rate  $c$  and residual elongation in each FRCC material. It can be seen in **Fig. 15** that after 28 days the recovery rate of the FRCC (SC) was almost zero or even minus. This could be because the self-healing products were not attached to the crack surface and steel cords were corroded during 28 days.

In the case of FRCC (PE), the recovery rate  $c$  is plotted over 0 and under 100. The tensile strength after self-healing didn't reach the first tensile strength, but could reach the first unloading stress. This could be because a lot of calcium carbonate crystals attached to many fibres. This indicated that, if the calcium carbonate crystals attach to the crack surface, the tensile strength after self-healing can be recoverable. Moreover it can also be seen in **Fig. 15** that the strength recovery rate becomes higher as residual elongation is smaller.

In the case of HFRCC, the recovery rate was higher than 100 when the residual elongation was less than even 2mm. It means that the tensile strength after self-healing could reach not only the first unloading stress, but also the first tensile strength. This could be because, as well as FRCC (PE), a lot of calcium carbonate crystals attached to crack surface with very fine fibres. Moreover the bond property of the steel cord damaged by pull out stress might be recovered by the self-healing products.

**Figure 16** shows a comparison of crack surfaces after the second tension test. By observing the crack surface, it was confirmed that corrosion of steel cord was observed not only on the surface of specimens with crack but also on the surface of inside of the crack in case of FRCC (SC). In case of HFRCC, however, the corroded steel fibre was observed only on the surface of the specimen (i.e. the external surface of the crack) but it was not observed on the internal surface of the crack. This could be because in HFRCC a lot of calcium carbonate crystals not only covered the surface of the crack but also attached to the matrix around steel cord fibres. It corresponds to the increase of tensile strength of HFRCC after the self-healing.

#### 4.5 The measurement of hydration degree

In order to make sure whether this difference of tensile strength healing is due only to the crystallization of calcium carbonate or the difference of the hydration degree of each FRCC has any effects on the difference of tensile strength healing, the hydration degree of each FRCC was measured. The measurement of hydration degree was done by mean of the backscattered electron image (Igarashi *et al.* 2004) as shown in **Fig. 17**. The backscattered electron image was converted to a binary image on each divided constituent phase and the volume fraction of the constituent phase was measured. By use of this volume fraction, the hydration degree of FRCC was calculated as follows.

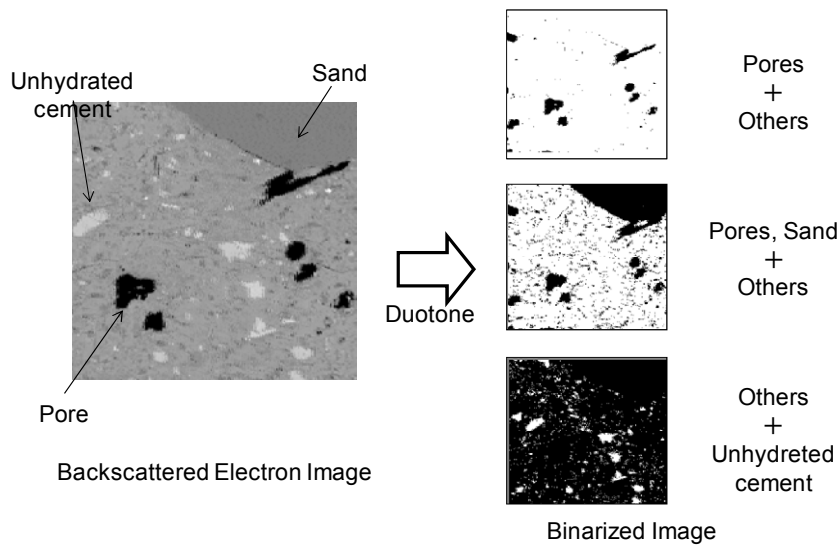


Fig. 17 Backscattered electron image of FRCC(PE).

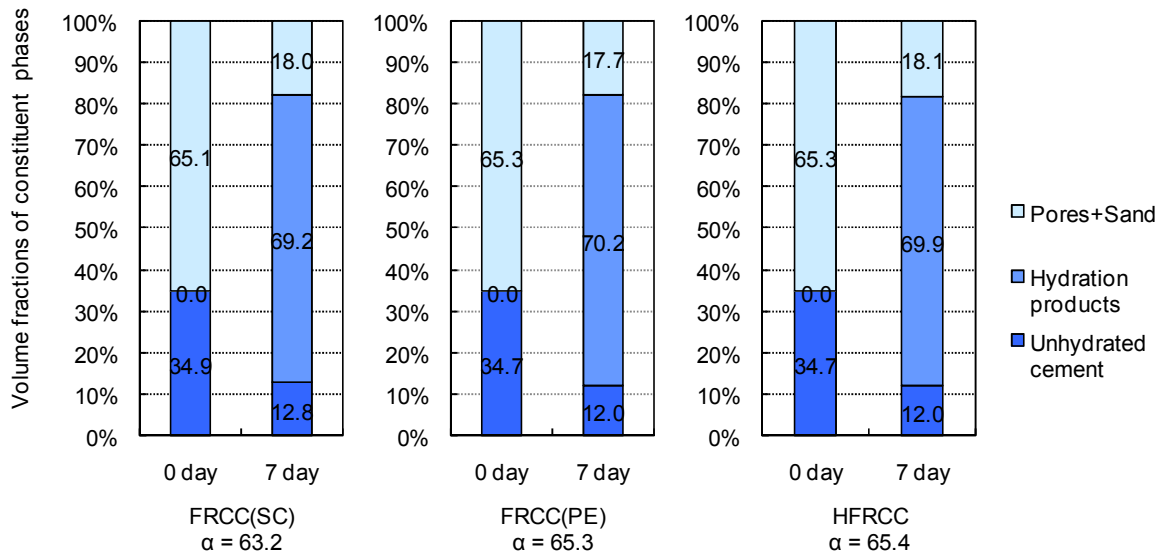


Fig. 18 Volume fractions of constituent phases in each FRCC specimen.

$$\alpha = 1 - \frac{UH_i}{UH_0} \tag{7}$$

where  $UH_i$  is area fraction of unhydrated cement particle at the age of  $t_i$ ;  $UH_0$  is the initial area fraction of unhydrated cement particles.

In Fig. 18, volume fractions of constituent phases and the hydration degrees in each FRCC specimen are shown. The hydration degree of each FRCC shows about 65% and there was no change in the hydration degree of each FRCC. Therefore it could be shown that the influence of the hydration degree difference of each FRCC on the tensile strength healing was little. It means that the dominant source of the self-healing is the crystallization of calcium carbonate.

### 5. Conclusions

This paper presented some results of an experimental study on the self-healing capability of the fibre reinforced cementitious composites. Based on the experimental study, the following conclusions were obtained:

- 1) Self-healing of cracks in FRCC materials was confirmed.
- 2) In the case of FRCC containing a lot of very fine fibres such as polyethylene, the formation of self-healing products becomes easy to be attached to the crack surface due to the tight space between fibres.
- 3) The self-healing products were confirmed to be calcium carbonate crystals by means of raman spectroscopy analysis.

- 4) The self-healing by calcium carbonate crystals leads to reducing water permeability and recovery of tensile strength.
- 5) By combining polyethylene fibre and steel cord in a FRCC (i.e. HFRCC), the tensile strength after the self-healing was recovered most significantly.

### Acknowledgement

The authors would like to express their thanks for the financial support by Grant-in-Aid for Scientific Research of Japan Society for the Promotion of Science (Project No. 18206058).

### References

- Dick-Nielsen, L., Stang, H. and Poulsen, P. N. (2007). "Micro-mechanical analysis of fibre reinforced cementitious composites." *Journal of Advanced Concrete Technology*, 5(3), 373-382.
- Edvardsen, C. (1999). "Water permeability and autogenous healing of cracks in concrete." *ACI Materials Journal*, 96(4), 448-454.
- Fantilli, A. and Vallini, P. (2007). "A cohesive interface model for the pullout of inclined steel fibres in cementitious matrixes." *Journal of Advanced Concrete Technology*, 5(2), 247-258.
- Granger, S., Loukili, A., Pijaudier-Cabot, G. and Chanvillard, G. (2007). "Experimental characterization of the self-healing of cracks in an ultra high performance cementitious material: mechanical tests and acoustic emission analysis." *Cement and Concrete Research*, 37, 1-9.
- Heide, N. ter and Schlangen, E. (2007). "Self healing of early age cracks in concrete." *Proc. of the 1<sup>st</sup> Int. Conf. on Self Healing Materials*, Noordwijk am Zee, The Netherlands, 1-12.
- Homma, D., Mihashi, H., Nishiwaki, T. and Mizukami, T. (2008a). "Experimental study on the self-healing capability of fibre reinforced cementitious composites." *Creep, Shrinkage and Durability Mechanics*, T. Tanabe *et al.* (eds.), CRC Press, 1, 769-774.
- Homma, D., Mihashi, H. and Nishiwaki, T. (2008b). "Experimental study of the self-healing capability of fiber reinforced cementitious composites." *Fibre Reinforced Concrete: Design and Applications*, R. Gettu (ed.), RILEM Publications, S.A.L. 1029-1038.
- Igarashi, S., Kawamura, M. and Watanabe, A. (2004). "Analysis of cement pastes and mortars by a combination of backscatter-based SEM image analysis and calculations based on the Powers model." *Cement and Concrete Composite*, 26, 977-985.
- Kanda, T. and Li, V. C. (2006). "Practical design criteria for saturated pseudo strain hardening behaviour in ECC." *Journal of Advanced Concrete Technology*, 4(1), 59-72.
- Kawamata, A., Mihashi, H. and Fukuyama, H. (2003). "Properties of hybrid fibre reinforced cement-based composites." *Journal of Advanced Concrete Technology*, 1(3), 283-290.
- Kimura, H., Ishikawa, Y., Kambayashi, A. and Takatsu, H. (2007). "Seismic behaviour of 200 MPa ultra-high-strength steel-fibre reinforced concrete columns under varying axial load." *Journal of Advanced Concrete Technology*, 5(2), 193-200.
- Li, V. C. (2003). "On engineered cementitious composites (ECC) - a review of the material and its applications." *Journal of Advanced Concrete Technology*, 1(3), 215-230.
- Li, V. C., Lim, Y. M. and Chan, Y.-W. (1998). "Feasibility study of a passive smart self-healing cementitious composite." *Composites- Part B*, 29B, 819-827.
- Mihashi, H. and Kohno, Y. (2007). "Toughening mechanism of hybrid fiber reinforced cement composites." *Fracture Mechanic of Concrete and Concrete Structures – High Performance Concrete, Brick Masonry and Environmental Aspects*, A. Carpinteri *et al.* (eds.), Taylor & Francis, 3, 1329-1339.
- Nishiwaki, T. and Mihashi, H. (2003). "Investment of self-healing function to high performance fibre reinforced cementitious composite." *Cement Science and Concrete Technology*, 58, 493-500. (in Japanese)
- Qian, S. and Li, V. C. (2007). "Simplified inverse method for determining the tensile strain capacity of strain hardening cementitious composites." *Journal of Advanced Concrete Technology*, 5(2), 235-246.
- Qian, S. and Li, V. C. (2008). "Simplified inverse method for determining the tensile properties of strain hardening cementitious composites (SHCC)." *Journal of Advanced Concrete Technology*, 6(2), 353-363.
- Ramm, W. and Biscopig, M. (1998). "Autogenous healing and reinforcement corrosion of water-penetrated separation cracks in reinforced concrete." *Nuclear Engineering and Design*, 179, 191-200.
- Reinhardt, H. W. and Jooss, M. (2003). "Permeability and self-healing of cracked concrete as a function of temperature and crack width." *Cement and Concrete Research*, 33, 981-985.
- Sharma, U., Bhargava, P., Singh, S. P. and Kaushik, S. K. (2007). "Confinement reinforcement design for plain and fibre reinforced high strength concrete columns." *Journal of Advanced Concrete Technology*, 5(1), 113-127.
- Sugano, S., Kimura, H. and Shirai, K. (2007). "Study of new RC structures using ultra-high strength fiber-reinforced concrete (UFC) – the challenge of applying 200 MPa UFC to earthquake resistant building structures." *Journal of Advanced Concrete Technology*, 5(2), 133-147.
- Tsukamoto, M. and Woener, J. D. (1991). "Permeability of cracked fibre-reinforced concrete." *Darmstadt Concrete*, 6, 123-135.
- Yang, E.-H., Wang, S., Yang, Y. and Li, V. C. (2008).

“Fibre-bridging constitutive law of engineered cementitious composites.” *Journal of Advanced Concrete Technology*, 6(1), 181-193.

Yang, Y.-Z., Lepech, M. D. and Li, V. C. (2005).

“Self-healing of engineered cementitious composites

under cyclic wetting and drying.” *Proc. Int. Workshop on Durability of Reinforced Concrete under Combined Mechanical and Climatic Loads (CMCL)*, Qingdao, China, F. H. Wittmann *et al.* (eds.) 231-241.